Photoelectron-diffraction and photoelectron-holography study of a Ge(111) high-temperature surface phase transition

T. T. Tran, S. Thevuthasan,* Y. J. Kim,† G. S. Herman, D. J. Friedman,‡ and C. S. Fadley*,†
Department of Chemistry, University of Hawaii, Honolulu, Hawaii 96822
(Received 31 January 1992)

Further evidence for a reversible surface-disordering phase transition on Ge(111) occurring ~150 K below the bulk melting point of 1210 K has been found using Ge 3*p* x-ray photoelectron diffraction (XPD). Azimuthal XPD data at takeoff angles of $\theta=19°$ (including nearest-neighbor forward-scattering directions and yielding high surface sensitivity) and $\theta=55°$ (for which second-nearest-neighbor scattering directions and more bulk sensitivity are involved) show abrupt decreases in intensity of ~40% and ~30%, respectively, over the interval of 900–1200 K. Photoelectron holograms and holographic images of near-neighbor atoms at temperatures above and below the phase transition indicate an identical near-neighbor structure for all atoms present in ordered sites. These combined diffraction and holography data indicate that by 1200 K the top 1–2 double layers of Ge atoms are completely disordered.

Evidence for a reversible high-temperature surface phase transition on Ge(111) has been found previously by McRae *et al.*[1,2] using low-energy electron diffraction (LEED) and by Denier van der Gon *et al.*[3] using medium-energy ion scattering (MEIS). This transition occurs near 1060 K or about 150 K below the bulk melting point. From the LEED data, it has been proposed that this is not a surface-melting or surface-roughening transition, but rather a disordering transition in which small laterally strained domains with a depth of one double layer [two Ge(111) monolayers] are produced.[1,2] However, beyond the suggestion based upon molecular mechanics modeling that there is a loss of registry between such strained domains and deeper layers,[1,2] no precise structural conclusions have been possible concerning the type of disorder involved. From the MEIS data, it has been proposed that an "incomplete melting" occurs, with the formation of a thin and uniform film of positionally disordered atoms on the Ge surface.[3] The depth of disordering has been observed to remain constant up to temperatures within 25 K of the melting point and estimated to be from 1 to 1.5 Ge(111) monolayers.

We have studied this system with x-ray photoelectron diffraction (XPD),[4] a surface structure probe that is primarily sensitive to short-range order in the first 3–5 shells of neighbors around each emitter[5] and thus of comparable range to MEIS, but much shorter in range than LEED. We have examined the Ge 3*p* photoelectron intensity from Ge(111) as a function of both the polar and azimuthal angles of emission and temperature. We also report results for this system obtained using a variant of XPD, photoelectron holography,[6–10] in which approximate direct imaging of atomic positions is achieved by a two-dimensional Fourier transform (FT) of large-scale data sets of intensity as a function of polar and azimuthal angles.

The XPD measurements were performed on a Vacuum Generators ESCALAB5 spectrometer modified for automated angle scanning;[11] Al $K\alpha$ radiation was used for excitation. Heating was done by a resistive button heater and temperatures were measured with an infrared pyrometer calibrated both by thermocouple and by passing through the melting point of Ge. The sample was a mirror-polished Ge wafer (*n*-type, Sb-doped, 5–30 Ω cm) oriented to within ±1.0° of (111). Surface cleaning involved sputtering (10^{-5} Torr Ar^+, 800 eV, 850 K, 45° off normal incidence, 20 min) and annealing (970 K, 30 min). This treatment was found to give a sharp $c(2\times8)$ LEED pattern at ambient temperature, although the $c(2\times8)$ reconstruction is known to disappear at 573 K or well below the transition we are studying.[1] Surface cleanliness was monitored by XPS core-level peaks, and no detectable contaminant peaks were found before or after a full series of diffraction or holographic data.

In the diffraction experiments, the azimuthal dependence of Ge 3*p* core-level intensities (kinetic energy = 1365 eV) was studied as a function of temperature from 300 to 1200 K. Azimuthal scans were performed at two polar angles of emission relative to the surface of $\theta=19°$ and 55°; the scattering geometry is shown in Fig. 1(a) and some of the diffraction curves are shown in Figs. 1(b) and 1(c). In the holographic experiments, full intensity profiles for Ge 3*p* were measured at 300, 970, and 1130 K. These profiles consisted of azimuthal scans with 1.8° steps over 80° in ϕ, which were then symmetry reflected to give the full 360° in azimuth; the polar angle θ was varied from grazing emission at $\theta=10°$ up to the normal at $\theta=90°$ in 1.8° steps.

The XPD results in Figs. 1(b) and 1(c) represent, respectively, azimuthal scans taken at 300, 800, and 1110 K and at 300, 840, and 1130 K, and at both (b) a surface-sensitive polar angle of 19° containing nearest-neighbor scattering directions and (c) a more bulk-sensitive polar angle of 55° containing next-nearest-neighbor scattering directions [cf. Fig. 1 (a)]. As temperature is increased, the diffraction peaks are significantly damped, although they do not significantly change their fine structure.

More specifically, comparing azimuthal scans in Fig. 1(b) taken at 800 and 1110 K (that is, just below and just above the expected transition point) the two main peaks at $\phi=0°$ (along the $[11\bar{2}]$ azimuth) and 60° (the $[\bar{1}2\bar{1}]$ azimuth) are found to be much reduced in both absolute and relative intensities. The fine structure between these two peaks, from about $\phi=14°$ to 52°, is also reduced in intensity, with only slight changes in its form. The absolute intensity of the peak along the $[11\bar{2}]$ azimuth decreases by ~40% from 800 to 1110 K. Furthermore, the overall anisotropy, which we measure as $(I_{max}-I_{min})/I_{max}=\Delta I/I_{max}$, decreases significantly from 0.36 to 0.29, or by 19% over the same interval. In Fig. 1(c), analogous results are plotted for emission at $\theta=55°$, and they lead to similar conclusions; the entire diffraction pattern is suppressed by ~30% in crossing the transition, with little change in fine structure. The overall anisotropy here decreases from 0.27 for the scan taken at 840 K to 0.24 for that taken at 1130 K, or by 11%.

In Fig. 2, we show more detailed intensity and background measurements as a function of temperature. The top panel in Fig. 2(a) shows the absolute background intensity under the $[11\bar{2}]$ forward-scattering peak at $\theta=19°$ corresponding to nearest-neighbor scattering [cf. Fig. 1(b)] and the bottom panel shows the absolute $[11\bar{2}]$ peak height (PH), both plotted as a function of temperature.

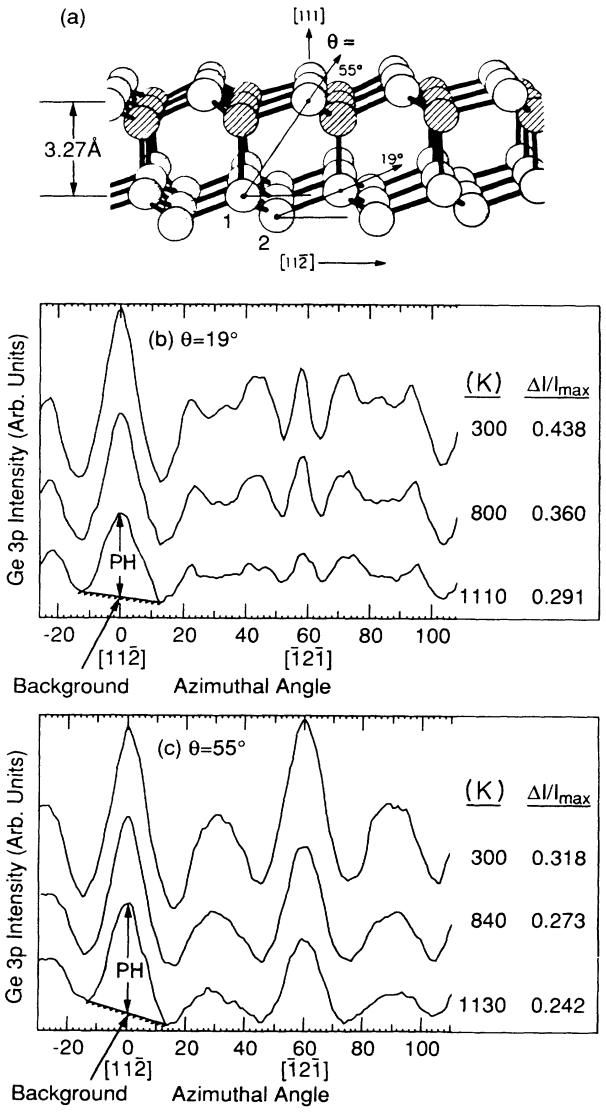

FIG. 1. (a) An unreconstructed Ge(111) surface showing nearest-neighbor and second-nearest-neighbor scattering directions at takeoff angles of $\theta=19°$ and 55° with respect to the surface; $\phi=0°$ ($[11\bar{2}]$ azimuth) for both of these directions. (b) Temperature-dependent azimuthal XPD data for Ge 3p emission from Ge(111) at 1365 eV and a low takeoff angle of $\theta=19°$. (c) As (b), but for a takeoff angle of $\theta=55°$.

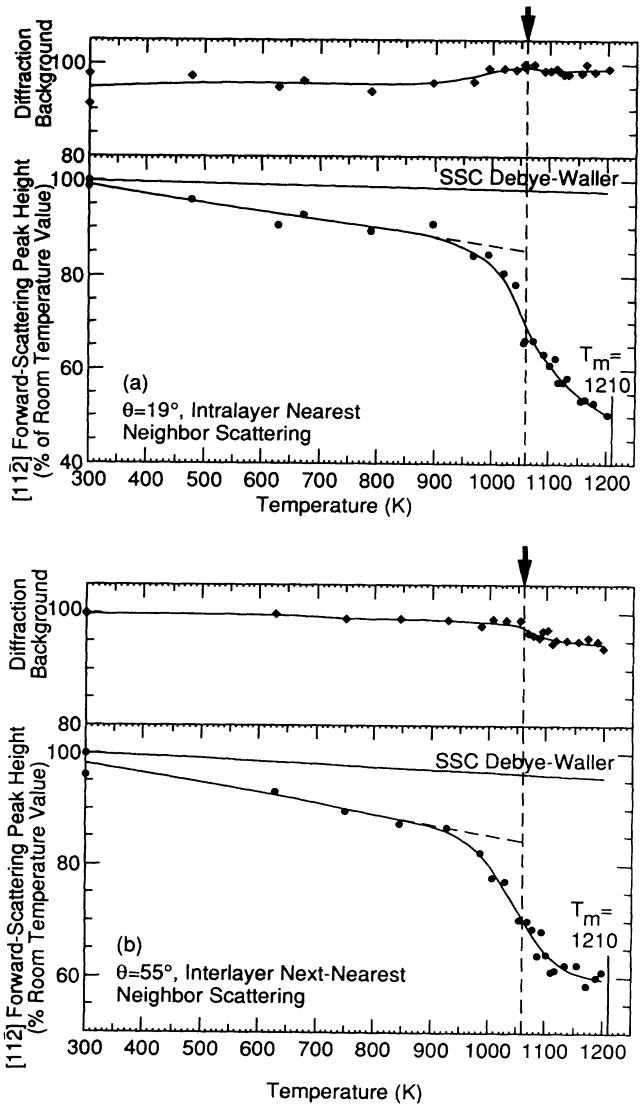

FIG. 2. (a) The temperature dependence of the height of the nearest-neighbor forwarding-scattering peak in Fig. 1(b) along $\theta=19°$, $\phi=0°$. Also shown are the temperature dependence of the background intensity under the forward scattering peak and the intensity expected on the basis of Debye-Waller effects in a single-scattering cluster model. (b) As (a), but for the next-nearest-neighbor forward-scattering peak in Fig. 1(c) along $\theta=55°$, $\phi=0°$.

In Fig. 2(b), analogous results are plotted for emission at $\theta=55°$. The points here were obtained with both increasing and decreasing temperature, and the form of the curve was found to be identical in both cases. It is thus clear that an abrupt and reversible drop of 43% in the diffraction intensity for $\theta=19°$ occurs over the interval 900–1200 K. A similar drop of 31% is seen for $\theta=55°$. By contrast, the background intensities at both θ values exhibit only very small, and probably statistically insignificant, deviations from constancy.

The drops in peak intensity at 1060 K cannot be explained by simple thermal vibrations. Debye-Waller (DW) effects are expected to yield a smooth and linear temperature dependence in the intensity of the forward-scattering peak, unlike the steplike transition observed. Model calculations of such a DW attenuation in a simple single-scattering cluster (SSC) approximation[12] are shown as the solid straight lines in Fig. 2. Thus, although such simple DW calculations are known to underestimate the attenuation of the forward-scattering peak height with temperature [an observation made previously in the analysis of XPD data from Cu(001) of Ref. 13], they at least qualitatively explain the experimental behavior below 900 K. However, the transition itself must be due to a larger-scale motion of the surface atoms, as proposed previously.[1,2]

We now ask what a holographic analysis of our data can add to this description of the phase transition. Our experimental data have been first analyzed according to a procedure previously described by Barton:[7] the three-dimensional intensity distribution $I(\mathbf{k})$ in the electron wave vector $\mathbf{k}$ with angles of emission θ and ϕ is converted to a normalized $\chi(\mathbf{k})$, where $\chi(\mathbf{k})=[I(\mathbf{k})-I_0(\mathbf{k})]/I_0(\mathbf{k})^{1/2}$, with the unscattered intensity $I_0(\mathbf{k})$ needed for normalization being obtained from polar-scan data for a heavily ion-bombarded surface in which no diffraction features were seen; this $\chi(\mathbf{k})$ is then projected onto the k_x,k_y plane with the average value of $\chi(\mathbf{k})$ set to zero, and, after multiplication by a phase factor $\exp(ik_z z)$ is Fourier transformed in k_x and k_y to yield what ideally is a cross section of the image in a plane at a distance z along [111] relative to a given emitter. Each intensity distribution or hologram occupies a cone centered along the $z=[111]$ axis, with a full angle given by $\alpha=160°$. In Figs. 3(a) and 3(b), we show the experimental $\chi(\mathbf{k})$ data for Ge(111) taken at temperatures of 970 and 1130 K, respectively (that is, just below and just above the disordering transition). Several low-index forward-scattering directions with the most dense rows of scattering atoms along them are labeled in Fig. 3(a). Similar $\chi(\mathbf{k})$ data were also measured at 300 K, but these are not shown due to length limitations; they were found to be very close to the results at 970 and 1130 K as to features and fine structure, as expected from Figs. 1(b) and 1(c).

Following a method suggested by Thevuthasan *et al.*[9] which has been shown to yield better subsequent FT image quality, we have multiplied the experimental $\chi(\mathbf{k})$ by a Gaussian function of the form $[1-\exp(-0.691\delta^2/\gamma^2)]$, where δ is the angular deviation of $\mathbf{k}$ from a given low-index forward-scattering axis and γ is a variable half-width at half-maximum intensity (HWHM). This function was applied to reduce the value of $\chi(\mathbf{k})$ along the highest-density $\langle 11\bar{1}\rangle$, $\langle 010\rangle$, $\langle 110\rangle$, and [111] directions, with a HWHM of 7.5° for all directions. This procedure reduces nonideal scattering anisotropy due to forward scattering.[9] Figures 3(c) and 3(d) show normalized images obtained after holographic inversion of the experimental data at 970 and 1130 K with Gaussian multiplication. The plane of these images at $z=3.27$ Å contains six nearest-neighbor atoms in the

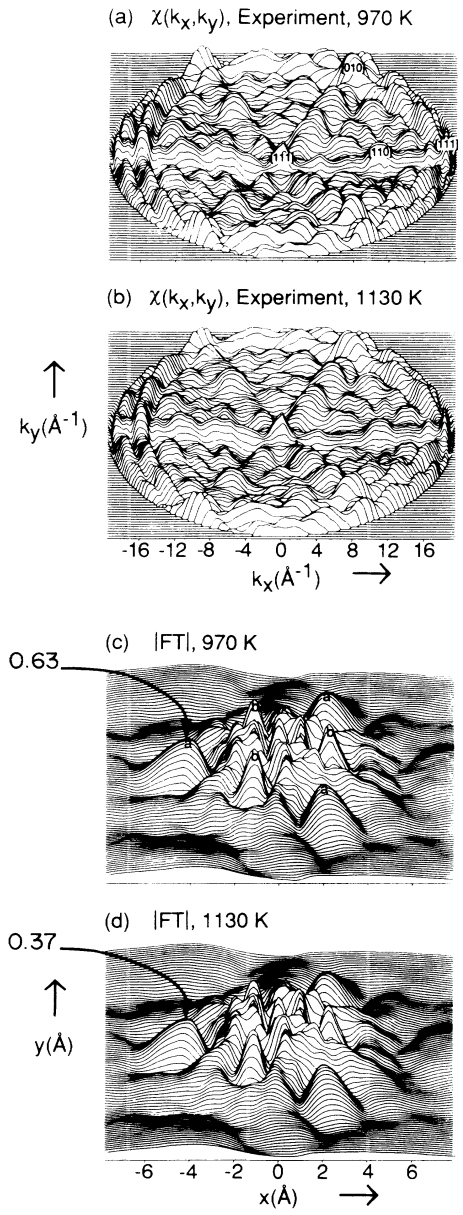

FIG. 3. (a) Projection of the experimental $\chi(\mathbf{k})$ for Ge(111) at 970 K onto the k_x-k_y plane. Several low-index directions are labeled. (b) As (a), but at 1130 K. (c),(d) Horizontal FT contour plots in the $z=3.27$ Å plane obtained with Gaussian removal of forward-scattering intensities along low-index directions in the initial $\chi(\mathbf{k})$ functions of (a) and (b). Contour plots are shown at (c) 970 K and (d) 1130 K.

first double layer above a given emitter of either type 1 or type 2 in Fig. 1(a); the positions of these neighbors are labeled "*a*" and "*b*." The relative intensity of the "*a*" peaks in these images are 1.0, 0.63, and 0.37 for 300, 970, and 1130 K, respectively, although the FT at 300 K is not shown. Once normalized, however, all the features observed at the three different temperatures become essentially identical, in particular for the two highest temperatures. These holographic near-neighbor images above and below the transition temperature thus indicate an identical near-neighbor structure for all atoms present in *ordered* sites.

Our data thus indicate no significant perturbation of the diffraction patterns (and thus also the near-neighbor geometries) associated with Ge atoms in ordered sites upon passing through the transition. The drops in diffraction peak intensities seen in Fig. 2 can in addition be explained by simple inelastic attenuation in a fully disordered, liquidlike overlayer. And the constancy of the backgrounds in Fig. 2 is consistent with no loss of diffuse intensity as the overlayer disorders, since the contribution to diffuse intensity from a given scattering atom should be very nearly the same whether it is in a lattice site or in a disordered configuration.

We can finally estimate the thickness of the disordered overlayer from the inelastic attenuation it produces on a diffraction peak intensity I upon passing through the transition: $I(\text{above})/I(\text{below})=\exp[-d/(\lambda_e \sin\theta)]$, where d is the overlayer thickness, λ_e is the inelastic attentuation length, and θ is the takeoff angle as defined previously. With values $I(\text{above})/I(\text{below})$ of approximately 0.57 for $\theta=19°$ and approximately 0.69 for 55° (cf. Fig. 2), and λ_c of 25 Å,[14] this yields $d=4.5$ Å or 1.4 double layers for $\theta=19°$ and $d=7.6$ Å or 2.3 double layers for $\theta=55°$. These numbers are thus in qualitative agreement with, but significantly larger than, the approximately 1.0 double layers derived from LEED (Refs. 1 and 2) and the 0.5–0.75 double layers derived from MEIS.[3]

This work was supported by the Office of Naval Research (Contract No. N00014-90-5-1457) and the U.S. Department of Energy (Contract No. DE-AC03-76SF00098).

---

*Present address: Department of Physics, University of California–Davis, Davis, CA 95616.

†Present address: Lawrence Berkeley Laboratory, Berkeley, CA 94720.

‡Present address: N.R.E.L., Golden, CO 80401.

[1]E. G. McRae and R. A. Malic, Phys. Rev. Lett. **58**, 1437 (1987); Phys. Rev. B **38**, 13 163 (1988).

[2]E. G. McRae, J. M. Landwehr, J. E. McRae, G. H. Gilmer, and M. H. Grabow, Phys. Rev. B **38**, 13 178 (1988).

[3]A. W. Denier van der Gon, J. M. Gay, J. W. M. Frenken, and J. F. van der Veen, Surf. Sci. **241**, 235 (1991).

[4]A preliminary account of this work based on lower-quality Ge 3*d* data appears in T. T. Tran, D. J. Friedman, Y. J. Kim, G. A. Rizzi, and C. S. Fadley, in *The Structure of Surfaces III,* edited by S. Y. Tong, M. A. van Hove, K. Takayanagi, and X. Xie (Springer-Verlag, Berlin, 1991), p. 522.

[5]C. S. Fadley, Phys. Scr. **T17**, 39 (1987); in *Synchrotron Radiation Research: Advances in Surface and Interface Science,* edited by R. Z. Bachrach (Plenum, New York, 1992).

[6]A. Szoeke, in *Short Wavelength Coherent Radiation: Generation and Applications,* edited by D. T. Attwood and J. Bokor, AIP Conf. Proc. No. 147 (AIP, New York, 1986).

[7]J. J. Barton, Phys. Rev. Lett. **61**, 1356 (1988); J. Electron Spectrosc. **51**, 37 (1990).

[8]G. R. Harp, D. K. Saldin, and B. P. Tonner, Phys. Rev. Lett. **65**, 1012 (1990).

[9]S. Thevuthasan, G. S. Herman, A. P. Kaduwela, R. S. Saiki, Y. J. Kim, W. Niemczura, M. Burger, and C. S. Fadley, Phys. Rev. Lett. **67**, 469 (1991).

[10]G. S. Herman, S. Thevuthasan, T. T. Tran, Y. J. Kim, and C. S. Fadley, Phys. Rev. Lett. **68**, 650 (1992).

[11]J. Osterwalder, M. Sagurton, P. J. Orders, C. S. Fadley, B. D. Hermsmeier, and D. J. Friedman, J. Electron Spectrosc. Relat. Phenom. **48**, 55 (1989).

[12]D. J. Friedman and C. S. Fadley, J. Electron Spectrosc. Relat. Phenom. **51**, 689 (1990).

[13]R. Trehan and C. S. Fadley, Phys. Rev. B **34**, 6784 (1986).

[14]S. A. Chambers, J. Vac. Sci. Technol. A **7**, 2459 (1989).

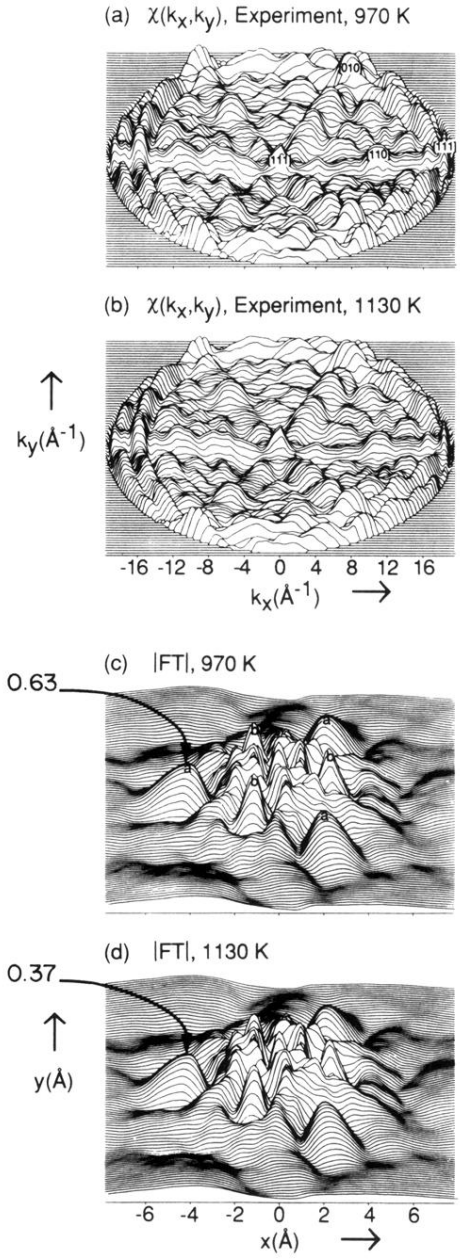

FIG. 3. (a) Projection of the experimental $\chi(\mathbf{k})$ for Ge(111) at 970 K onto the k_x-k_y plane. Several low-index directions are labeled. (b) As (a), but at 1130 K. (c),(d) Horizontal FT contour plots in the $z = 3.27$ Å plane obtained with Gaussian removal of forward-scattering intensities along low-index directions in the initial $\chi(\mathbf{k})$ functions of (a) and (b). Contour plots are shown at (c) 970 K and (d) 1130 K.